GEOMETRIC AND MATERIAL NONLINEAR ANALYSIS OF REINFORCED CONCRETE SLABS AT FIRE ENVIRONMENT

Dr. Ayad A. Abdul -Razzak
Assistant Professor
Civil Eng. Dept.- Mosul University

ABSTRACT

In the present study a nonlinear finite element analysis is presented to predict the fire resistance of reinforced concrete slabs at fire environment. An eight node layered degenerated shell element utilizing Mindlin/Reissner thick plate theory is employed. The proposed model considered cracking, crushing and yielding of concrete and steel at elevated temperatures. The layered approach is used to represent the steel reinforcement and discretize the concrete slab through the thickness. The reinforcement steel is represented as a smeared layer of equivalent thickness with uniaxial strength and rigidity properties.

Geometric nonlinear analysis may play an important role in the behavior of reinforced concrete slabs at high temperature. Geometrical nonlinearity in the layered approach is considered in the mathematical model, which is based on the total Lagrangian approach taking into account Von Karman assumptions.

Finally two examples for which experimental results are available are analyzed, using the proposed model .The comparison showed good agreement with experimental results.

KEYWORDS: Fire resistance, Material and Geometrical nonlinearity, Reinforced Concrete Slabs

INTRODUCTION

Research of the fire effect on concrete, steel and reinforced concrete structures has been conducted since at least 1922 (as shown by Schneider)[1] The main areas of interest are[2] the understanding of the complex behavior of the material itself, and the structural safety and integrity of the building during and after the fire. The thermal and structural analysis are interfaced and not integrated. In other words, the temperatures distribution within the structural element due to temperature rise is first calculated for the entire duration of temperature exposure, and then fed into the structural analysis program to produce the stresses and strains for the structures[2].

Nizamuddin and Bresler[3] presented a nonlinear finite element computer program FIRES-SL for the analysis of reinforced concrete slabs at fire. The analysis based on Kirchhoff thin plate theory and includes the coupling of bending and membrane action. Borst and Peeters[4] developed an algorithm which simultaneously considers the effects of thermal dilatation, degradation of the elastic properties with increasing temperature, transient thermal strain, and smeared cracking to simulate plain and reinforced concrete at high temperatures. Results of the presented model show a good agreement with experimental tests for both plain and reinforced concrete models. Huang et al[5] developed a nonlinear finite element approach to enable practical modeling of fairly large composite steel/concrete frames under the influence of compartment fire and external loading. Again the validity of the proposed models shows a good agreement with experimental results.

Ahmed and Al-Zubaedi[6] used the finite difference method to study the nonlinear structural behavior of reinforced concrete plates. Large deflection theory and dynamic relaxation technique were used to calculate the strains and stresses in the plate at elevated temperature.

Ahmed and Hasan[7] studied the effect of cyclic heating and cooling on the nonlinear behavior of reinforced concrete slabs at different load conditions before and after cracking up to failure. Finite difference method with dynamic relaxation technique were used in the solution of the differential equations.

Abdul-Razzak and Said[8] used nonlinear finite element analysis to simulate the fire resistance of reinforced concrete slabs at elevated temperatures. An eight node layered degenerated shell element utilizing Mindlin/Reissner thick plate theory with initial stiffness technique was employed. The proposed model considered cracking, crushing, and yielding of concrete and steel at high temperatures. The validation of the proposed models are examined against experimental data of previous researches and showed good agreement.

Analysis of reinforced concrete slabs at elevated temperatures consists of two problems, heat and structural response. Heat flow problem involves type of exposure (intensity and duration), temperature distribution within the slab thickness, there are many ways of exposing concrete structures to elevated temperatures. The most common types of exposures is by an accidental fire in a building. Normally fire intensity (temperature levels and duration) depends on the combustible materials, opening factor, types, and shapes of the structure. The standard fires curves used in testing, analysis, and design have different growing rate, duration, and peak temperature depending upon its application area (i.e. building, offshore/petrochemical, tunnels)[2]. For example, the Rijs Water Staat (RWS) Dutch fire models which is intended to simulate tankers carrying petrol in tunnels is rapidly exceeds 1200 ^{o}C and peaking 1350^{o}C (melting temperature of concrete)[2]. While the standard ISO834 is the most common fire model used in the analysis and design of members at elevated temperatures, which has a slower growing rate and lesser peak temperature. Temperature distribution within the slab thickness depends mainly on concrete heat conductivity, type of concrete and aggregate and their proportion in the mix. It has been found that steel reinforcement has a small effect on temperature distribution especially when its ratio below 0.04[9]. So their presence is often neglected in the thermal analysis of reinforced concrete slabs.

The structural response involves the behavior of reinforced concrete slabs which its constitutes were affected by temperature rise under the applied load. In the present work, the combined effect of the two responses is systematically

evaluated using computer software presented by Owen and Figueiras[10], in which degenerate quadratic thick shell elements employing a layered discretization through the thickness are adopted.

The software is modified in order to accommodate the evaluation of temperature exposure as well as the structural response. Geometric nonlinear analysis was also considered in the numerical model.

BASIC THEORY

Formulation of the standard degenerate shell element (Ahmad's element) is well known[11], and therefore only a brief description of the element will be presented here. The global displacements can be found from mid-surface nodal displacements (u_i, v_i, w_i) and the relative displacements are caused by the two rotations (α_i, β_i) of the normal as:

$$\begin{Bmatrix} u \\ v \\ w \end{Bmatrix} = \sum_{i=1}^{n} N_i \begin{Bmatrix} u_i \\ v_i \\ w_i \end{Bmatrix}_{mid} + \sum_{i=1}^{n} N_i \zeta \frac{h_i}{2} [v_{1i} - v_{2i}] \begin{Bmatrix} \alpha_i \\ \beta_i \end{Bmatrix} \quad \ldots\ldots\ldots\ldots\ldots (1)$$

where (v_{1i}, v_{2i}) are unit vectors and (n) is the number of nodes.

or simply

$$\{u\} = \sum_{i=1}^{n} [N_i]\{\delta_i\} \quad \ldots\ldots (2)$$

The strain matrix [*B*] (of order 5 by the total degrees of freedom of the element), relating the strain nodal variables.

$$\{\varepsilon\} = [B]\{\delta\} \quad \ldots\ldots\ldots\ldots\ldots (3)$$

where

$$\{\delta\} = [u, v, w, \alpha, \beta]^T \quad \ldots\ldots (4)$$

and the five stress components in the local coordinates system are,

$$\{\sigma\} = [D](\{\varepsilon\} - \{\varepsilon_\circ\}) \quad \ldots\ldots\ldots\ldots (5)$$

where $\{\varepsilon_\circ\}$ may represent any initial strains such as the expansion due to thermal load. In the present code the strain matrix [B] is calculated at the mid-surface of each layer; the element stiffness matrix $[K^e]$ and the internal force vectors $\{f^e\}$ are thus defined as follows:

$$[K^e] = \int_{-1}^{+1}\int B^T D B J \, d\zeta \, dA \quad \ldots\ldots (6)$$

$$\{f^e\} = \int_{-1}^{+1}\int B^T \sigma J \, d\zeta \, dA \quad \ldots\ldots\ldots (7)$$

where

$$\int dA = \int_{-1}^{+1}\int_{-1}^{+1} d\xi \, d\eta \qquad \ldots\ldots\ldots\ldots (8)$$

(Integration on layer mid-surface)

MATERIAL CONSTITUTIVE RELATIONSHIPS AT ELEVATED TEMPERATURE

1. Biaxial Concrete State

At present, there is still little data and few theoretical models available concerning the constitutive modeling of concrete under biaxial stress state at elevated temperatures[5]. Therefore in this paper the failure envelope at ambient temperature is extended to elevated temperature taking into account the changes into its related parameters with temperature rise. So at each temperature level there is a failure envelop having the same characteristics of the failure envelope at ambient temperature. The formulation of the failure envelope proposed by Hinton and Owen [10]which is slightly differs from Kupfer et al[12] was adopted in the present study, the yield condition for the slabs can be written in terms of the stress components as:

$$f(\sigma)=\{1.355[(\sigma x2+\sigma 2y-\sigma x\sigma y)+3(\tau xy2+\tau xz2+\tau yz2)]+0.355\sigma o(\sigma x+\sigma y)\}1/2=\sigma o \qquad \ldots\ldots(9)$$

where (σo) is the equivalent effective strength taken as compressive strength (f_{ct}) obtained from Fig.(2).

2. Modulus of Elasticity

At elevated temperature a decrease in modulus of elasticity is mostly affected by the aggregate types[13]. The relationship between the modulus of elasticity and temperatures rise used in the present study shown in Fig.(1) and used by Said[14] and indicates almost a constant rate of decrease in elasticity with increasing temperatures.

3. Uniaxial Compressive Strength of Concrete

As shown by many researches, the concrete compressive strength deteriorate with temperature rise, the rate of deterioration varies considerably with temperature levels. The model in Fig. (2) Used by Said[14] for the relationship between compressive strength and temperature rise being considered in the present study.

4.Tensile Strength

There is paucity of experimental data with regard to the dependence of concrete tensile strength with temperature, Fig. (3) shows the model used by Said [14]

and being considered in the present

study. Furthermore a gradual release of the concrete stress component normal to the cracked plane has been used to model the tension stiffening phenomena[10]. Unloading and reloading of cracked concrete is assumed to follow the linear behavior shown with a fictitious elasticity modulus Ei given by:

$$E_i = \alpha \ f_t^{'}(1-\varepsilon_i / \varepsilon_m) / \varepsilon_i$$
$$\varepsilon_t \le \varepsilon_i \le \varepsilon_m \qquad \ldots\ldots\ldots\ldots\ldots (10)$$

where (α, ε_m) are parameters of tension stiffening, $(f_t^{'})$ is the tensile strength, (ε_t) is the tensile strain at $(f_t^{'})$, and (ε_i) is the maximum tensile strain value reached at the point considered. The normal stress $(\sigma_1 \ or \ \sigma_2)$ can be obtained by the following expression,

$$\sigma_1 = \alpha \ f_t^{'}(1-\varepsilon_1 / \varepsilon_m)$$
$$\varepsilon_t \le \varepsilon_1 \le \varepsilon_m \qquad \ldots\ldots\ldots\ldots\ldots (11)$$

or by

$$\sigma_1 = \sigma_i \varepsilon_1 / \varepsilon_i$$
$$\varepsilon_1 < \varepsilon_i \qquad \ldots\ldots\ldots\ldots\ldots (12)$$

5. Poisson's Ratio

As reported by many researches[1], the results of relation between Poisson's ratio and temperature increase are erratic and no general trend of effect of temperature was clearly evident. As a result a constant value of 0.19 of Poisson's ratio at all temperature levels is adopted in the present research.

6. Concrete Strain

The crushing failure of concrete is a strain-controlled phenomenon. A simple way is used by converting the yield criterion in stresses into the yield criterion directly in terms of the strain, thus crushing condition can be expressed in terms of the total strain components as:

$$1.355\,[(\varepsilon x^2+\varepsilon^2 y-\varepsilon x\varepsilon y)+0.75(\gamma xy^2+ \gamma xz^2+\gamma yz^2)]+0.355\varepsilon u(\varepsilon x+\varepsilon y) = \varepsilon u^2$$

When Equation (13) is satisfied, the strain (εu) reaches the crushing surface, and the concrete is assumed to lose all its characteristics of strength and stiffness.

A single unique relation between strain and temperature reported by Schneider [1] as shown in Fig.(4) is used by Said[14] and adopted in the present study

7. Steel Reinforcement

Steel reinforcement behavior in tension and compression is modeled by considering the steel bars as layers of equivalent thickness. Each steel layers exhibits uniaxial response, having strength

and stiffness characteristics in the bar direction. A bilinear idealization is adopted in order to model the elasto-plastic stress-strain relationships. The properties of reinforcement (yield strength and modulus of elasticity) are presented in Figs. (5 and 6)[15].

GEOMETRIC NONLINEARITY

The causes of structural nonlinearities may be broadly classified in two groups: material and geometric. The various aspects of material nonlinear behavior of a structure, under the assumptions of small displacement. The problem of geometrically nonlinear behavior is usually tackled by tracing the geometrical change of both the structure and its elements in a step- by –step manner.

The strain components can be divided into components, first is a linear strain $\{\varepsilon\}_o$ and the second is a nonlinear strain $\{\varepsilon\}_L$.

$$\{\varepsilon\} = \{\varepsilon\}_o + \{\varepsilon\}_L \quad \ldots\ldots\ldots\ldots (14)$$

and

$$d\{\varepsilon\} = d\{\varepsilon\}_o + d\{\varepsilon\}_L \quad \ldots\ldots\ldots\ldots (15)$$

The strain-displacement matrix can be divided into two parts,

$$[B] = [B]_o + [B]_L \quad \ldots\ldots\ldots\ldots (16)$$

where $[B]_o$ is the linear part of strain-displacement matrix.

$[B]_L$ Is the nonlinear part of strain-displacement matrix.

The nonlinear components of the strain vector can be expressed as follows[10]:

$$\{\varepsilon\}_L = \begin{Bmatrix} \frac{1}{2}(\frac{\partial W'}{\partial X'})^2 \\ \frac{1}{2}(\frac{\partial W'}{\partial Y'})^2 \\ \frac{\partial W'}{\partial X'}\frac{\partial W'}{\partial Y'} \\ 0 \\ 0 \end{Bmatrix} = \frac{1}{2}\begin{bmatrix} \frac{\partial W'}{\partial X'} & 0 \\ 0 & \frac{\partial W'}{\partial Y'} \\ \frac{\partial W'}{\partial Y'} & \frac{\partial W'}{\partial X'} \\ 0 & 0 \\ 0 & 0 \end{bmatrix} \begin{Bmatrix} \frac{\partial W}{\partial X'} \\ \frac{\partial W'}{\partial Y'} \end{Bmatrix} \quad \ldots\ldots\ldots\ldots (17)$$

Or

$$\{\varepsilon\}_L = \frac{1}{2}[S]\ \{T\} \quad \ldots\ldots\ldots\ldots..(18)$$

where

$$[S]^T = \begin{bmatrix} \frac{\partial W'}{\partial X'} & 0 & \frac{\partial W'}{\partial Y'} & 0 & 0 \\ 0 & \frac{\partial W'}{\partial Y'} & \frac{\partial W'}{\partial X'} & 0 & 0 \end{bmatrix}$$

……(19)

The vector{ T }can be defined

$$\{T\} = \begin{Bmatrix} \frac{\partial W'}{\partial X'} \\ \frac{\partial W'}{\partial Y'} \end{Bmatrix} = [G]\ \{a\} \quad \ldots\ldots\ldots\ldots(20)$$

The term $[G]$ is the matrix with two rows and a number of columns equal to the total number of element nodal variables.

The geometrical stiffness matrix which can be written as,

$$[K]_\sigma = \int_V [G]^T \{\sigma\} [G] \, dv \qquad \text{……..(21)}$$

In which the matrix $[G]$ has been defined previously from Eq. (20) and $\{\sigma\}$ is the components of the Piola- Kirchhoff stress vector.

STRUCTURAL RESPONSE AND FINITE ELEMENT DISCRITIZATION

Structural response is defined in terms of transient deformations, forces, moments, and material degradation (cracking, crushing, and yielding) throughout the slab. These factors account for material behavior at varying temperatures, including dimensional changes caused by temperature variation, changes in mechanical properties with changes in temperature, degradation of section through cracking and crushing, and inelastic deformations associated with nonlinear stress, strain characteristics. An eight node thick shell Ahmad element with layer model which subdivide the slab into concrete and steel layers to allow the consideration of temperature variation and the consequent materials properties through slab depth. Slabs are modeled as an assemblage of finite elements connected at nodal points, each elements are considered to be made up of number of layers representing plain concrete or reinforcing steel. Each layer can have a different temperature, but with same layer the temperature is constant, therefore material properties within each layer is uniform. The basic analytical problems is to determine the deformation history of the nodes r(t) when external loading at the nodes R(t) is applied while the temperature increases. A finite element method using nonlinear initial stiffness formulation coupled with time step integration is used to predict the structural response as shown in Fig. (7). A time step begins when a time increment Δti and external load increment ΔRi are read. These values are added to the previous time and load values to obtain the current time ti and load vector Ri.. The first iteration in a time step is initiated with the assumption that the current deformation ri is equal to the deformation at the end of

the previous time step r_i^{-1}. The current tangent stiffness kij and the current internal forces is calculated. If equilibrium not satisfied i.e., the difference between the external applied load and the internal forces greater than the permissible tolerance a correction deformation is calculated and added to the current deformation and thereby a more accurate deformation shape is determined. The iterative cycle is repeated, a new tangent stiffness and internal forces is calculated on the basis of the new deformation shape. Iteration continued until equilibrium is satisfied within the permissible tolerance.

NUMERICAL EXAMPLES

Example 1

For validation of the proposed model, a simply supported (4900 x 1900 mm) reinforced concrete slab subjected to fire test at University of Gent and analyzed by Brost and Peeters [4]is considered. The slab was simply supported on the short sides while the displacements at the other two sides were free. The slab thickness is 150 mm loaded by two jacks over the full width as shown in Fig.(8). Slab geometry, loading, and material properties are summarized in Table (1). Only one half of the slab was analyzed since both slab and the heated area were symmetrical. The slab response under the applied load at fire environment is presented in terms of time-deflection.

As shown in Fig.(9), the results of geometric nonlinear analysis, which is the present study, shows good agreement especially at the failure stage with experimental results better than the results of reference [8] in which the geometric nonlinear analysis is not considered. It also seen from Fig.(9) that there is differences between the present analysis results and the experimental results at the first stage of heating and this can be attributed to the neglecting of transient thermal strain in the present analysis which proved to take major part during the first heating stage of concrete[2].

Example 2

Another comparison made with full scale fire test on slab specimen tested by the PCA [3]as a part of a research program on the response of reinforced concrete slabs at fire. The slab was 2.7m square, 101.6 mm thick as shown in Fig.(10) reinforced with 10 mm steel bars top and bottom spaced at 150 mm in both directions. Slab material properties are

listed in Table (2). The central (840 mm x 840 mm) area of the slab was exposed to the ASTM E119 standard fire, the remaining portion of the slab was outside the furnace. The slab was supported vertically near the corners of the heated area while the outer edges were free. Since both the slab and the heated area were symmetry, only one-quarter of the slab is analyzed in the present analysis. The variation of central deflection with time is shown in Fig. (11). Very good agreement has been noticed between the experimental results and the present analysis especially at the final stage of heating. It is also seen from Fig.(11) that the results of geometric nonlinear analysis, which is the present study, is better than the results of reference[8] in which the geometric nonlinear analysis is not included.

CONCLUSIONS

In this paper models and algorithms have been presented for the analysis of reinforced concrete slabs at elevated temperatures. Models of concrete and steel behavior at elevated temperature are adopted form experimental studies of previous researches. These models are yet need to be further studied and developed especially for biaxial failure envelope of concrete, concrete tensile strength, and Poisson ratio.

It is concluded that the geometric nonlinear analysis incorporating the present model enhance the response of the deflection with time and plays an important role in determining the failure load of the slabs at elevated temperature.

REFERENCES

1. Schneider, U.,“ Concrete at high temperature _ A general review”, Fire Safety Journal, Vol. 13, 1988, pp. 55-68.

2. Khoury, G.A., “Effect of fire on concrete and concrete structures”, Progress in Structural Engineering and Materials , 2000, Vol.2, pp 429- 447 .

3. Zuhayer Nizamuddin, and Boris Bresler, “ Fire resistance of reinforced concrete slabs”, Journal of the Structural Division, Vol. 105, No. ST8, 1979, pp. 1653-1671.

4. Rene de Borst, and Peeters, P.J.M., “ Analysis of concrete structures under thermal loading”, Computer Methods in Applied Mechanics and Engineering, Vol. 77, 1989, pp. 293-310.

5. Zhaohui Huang, Ian W. burgess, and Roger J. Plank, “Nonlinear analysis of reinforced concrete slabs subjected to

fire", ACI Structural Journal, Vol. 96, No. 1, 1999.

6. Ahmed, A.H., and Al-Zubaedi, H., "Material and geometrical nonlinearity of reinforced concrete plates subjected to high temperature", AL-Rafidain Engineering Journal Vol.12, No.4, 2004 , pp. 16-34.
7. Ahmed, A.H., and Hasan, H.M.A., " Effect of cyclic heating on reinforced concrete thick slabs", AL-Rafidain Engineering Journal Vol.13, No.4, 2005 , pp. 35-51.
8. Abdul-Razzak, A.A., and Said, A.H., "Nonlinear Analysis of Reinforced Concrete Slabs at Elevated Temperature ", Send for Publication to AL-Rafidain Engineering Journal
9. Ellingwood, B., and Shaver, J.R., "Effect of fire on reinforced concrete members', Journal of the Structural Division, ASCE, Vol.106 No. ST11, November 1980, pp. 2151-2166.
10. Hinton , E and D. R. J. Owen , "Finite element software for plates and shells" , Pineridge Press , Swansea , 1984.
11. Ahmad, S., Irons, B.M., and Zienkiewicz, O.C., " Analysis of thick and thin shell structures by curved finite elements", Inter. J. Num. Meth. Engng. Vol.2, No.3, 1970, pp. 419-451.
12. Kupfer, H., Hilsdrof, H.K., and Rusch, H., "Behavior of concrete under biaxial stresses" ACI Journal, Vol. 106, No. 8, 1969, pp. 656-665.
13. Harada, T., Takeda, J., Yamanes, S., and Furumura, F., " Strength, elasticity, and thermal properties of concrete subjected to elevated temperatures", Concrete for Nuclear Reactors, SP-34, American Concrete Institute, Detroit, 1972, pp. 377-406.
14. Said, A.H., "Nonlinear analysis of reinforced concrete slabs at elevated temperatures" M.Sc. Thesis, University of Mosul 1999.
15. Holmes, M.A., Cook, R.D., and Crtok, G.M., " The effect of elevated temperatures on the strength properties of reinforcing and prestressing steels", The Structural Engineer, Vol. 60B, No.1, 1982, pp. 7-13.

Table (1) Material Properties and Reinforcement of Slab Shown in Fig.(8)

E MPa	f_C MPa	f_t MPa	υ	α $^oC^{-1}$	E_s MPa	f_{sy} MPa	Reinforcement $m\,m^2$	Self-weight kN/m^2	Load weight kN/m
45200	42.7	2.6	0.2	0.000012	215000	504	1178	6.29	14.5

Table (2) Material Properties of Slab Shown in Fig. (10)

E MPa	f_C MPa	f_t MPa	υ	α $^oC^{-1}$	E_s MPa	f_{sy} MPa
27590	32.35	5.17	0.19	0.000012	20700	415

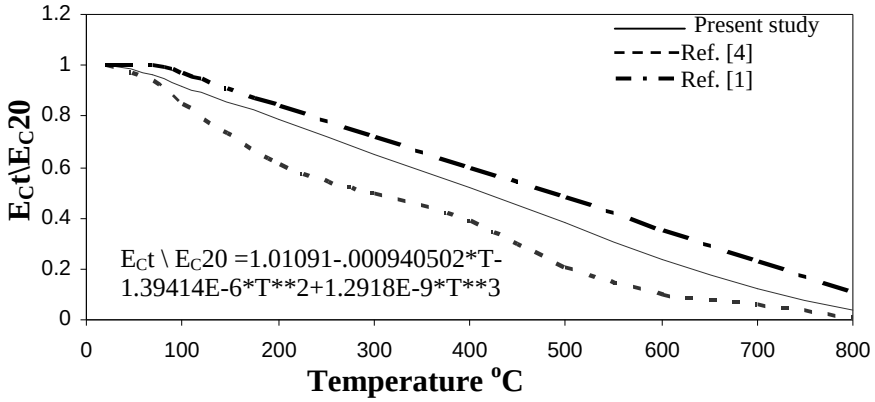

Fig(1). Variation of Concrete Modulus of Elasticity with Temperature Rise

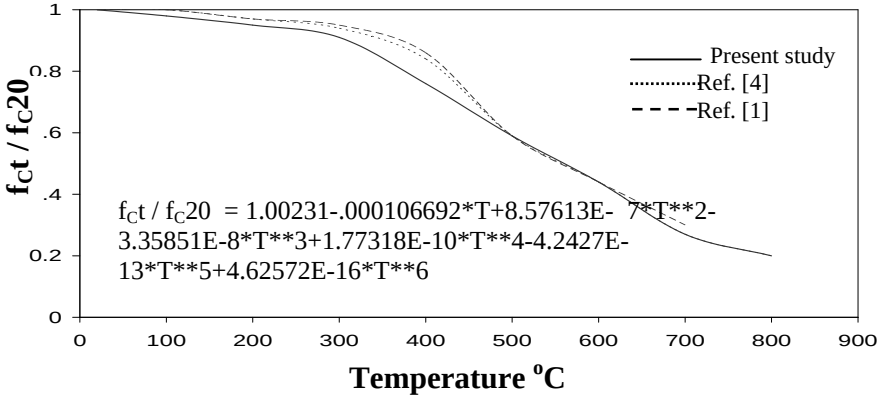

Fig(2). Variation of Concrete Compressive Strength with Temperature Rise

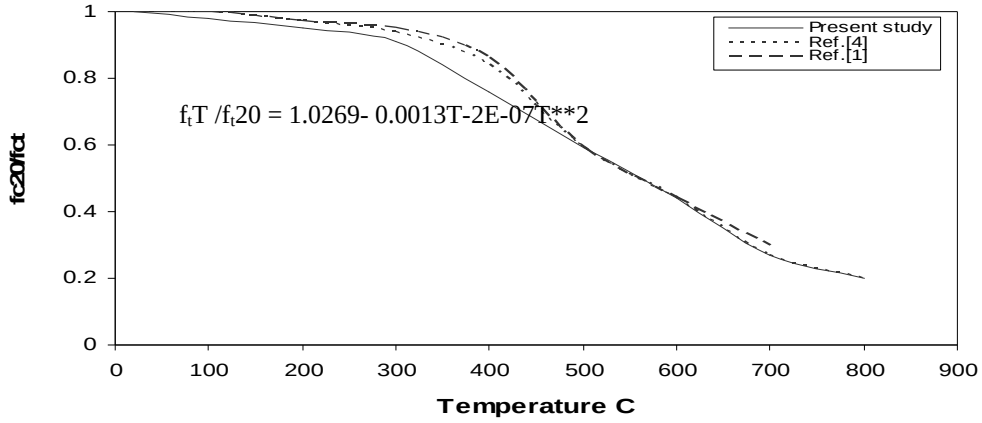

Fig(3). Variation of Concrete Tensile Strength with Temperature Rise

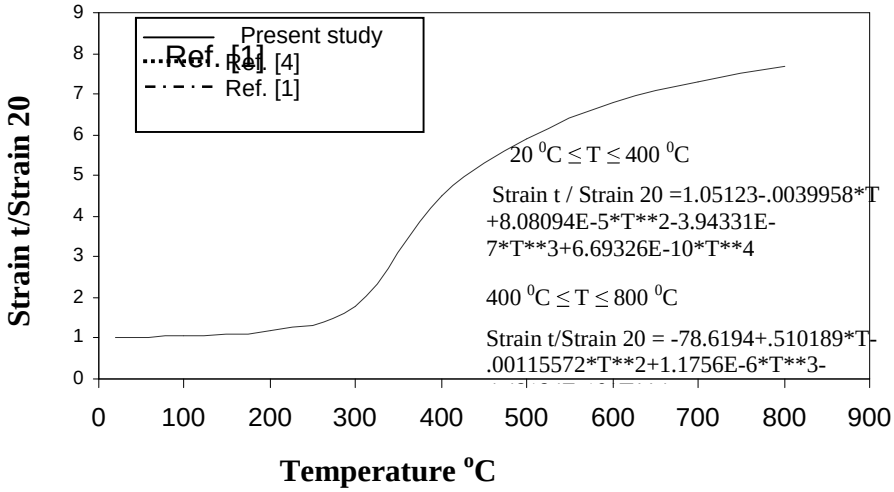

Fig(4). Variation of Concrete Strain with Temperature Rise

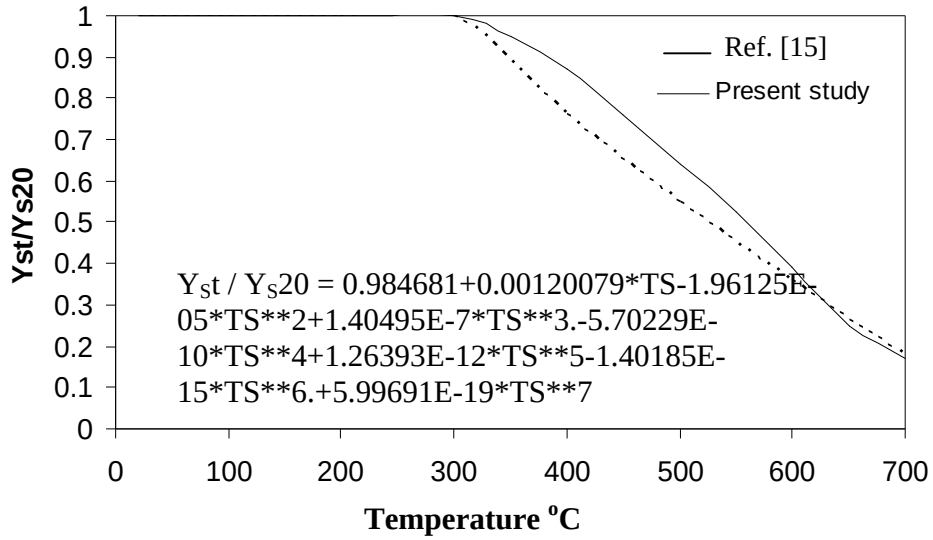

Fig(5). Variation of Steel Yield Strength with Temperature Rise

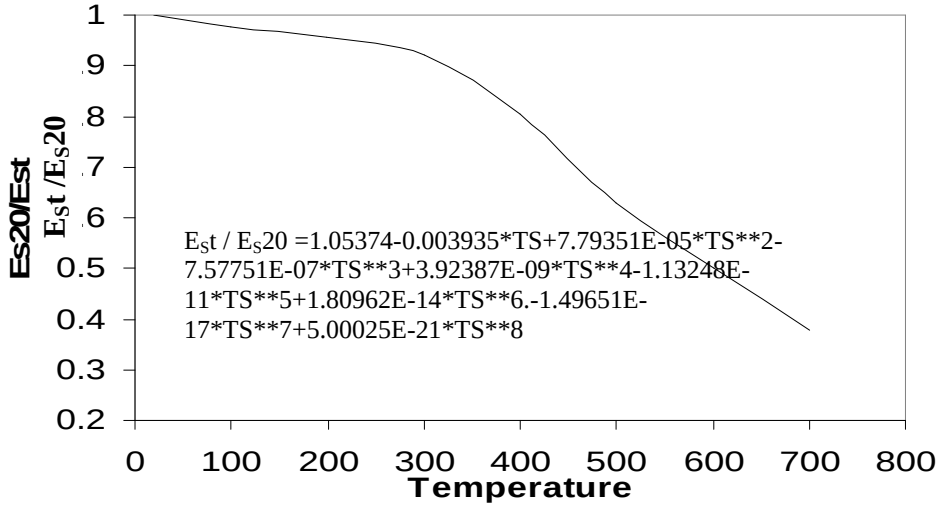

Fig(6). Variation of Steel Modulus of Elasticity with Temperature Rise

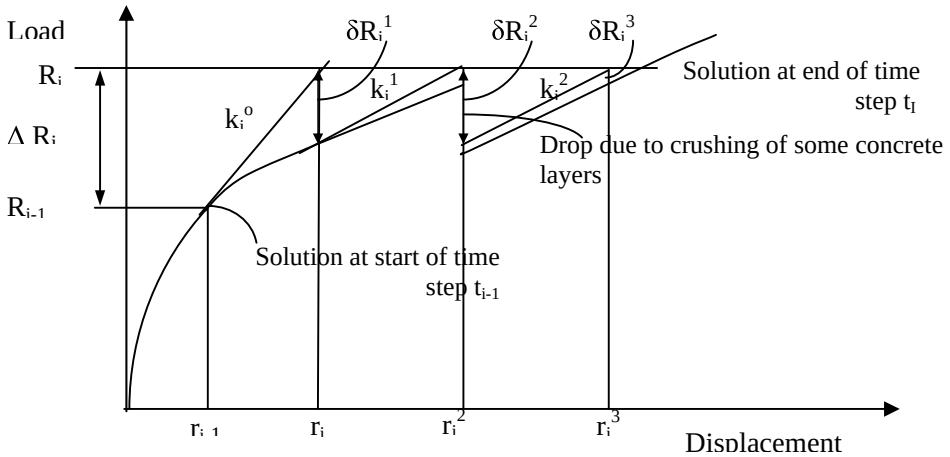

Fig.(7) Solution of Time Dependent Nonlinear Equilibrium Equation

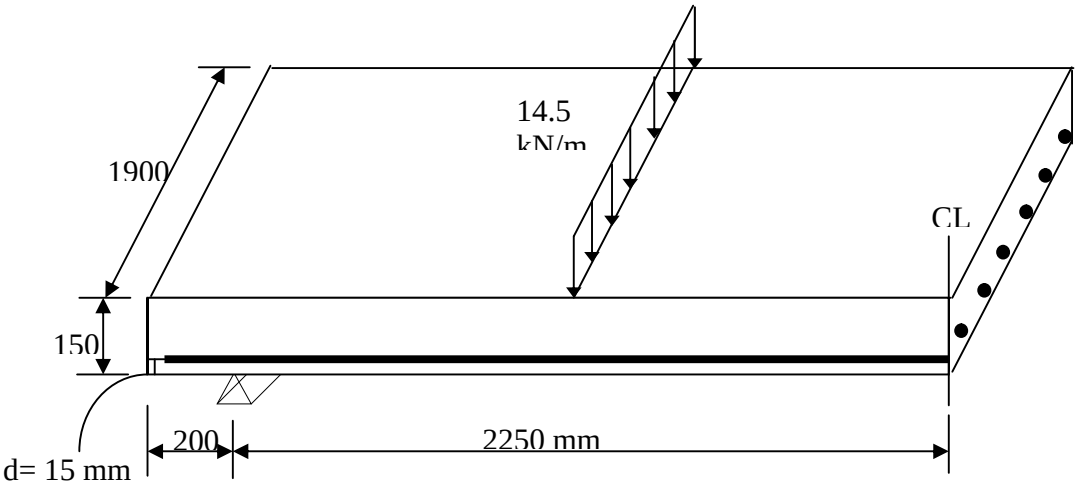

Fig.(8) - Slab Analyzed by De.Borst [4].

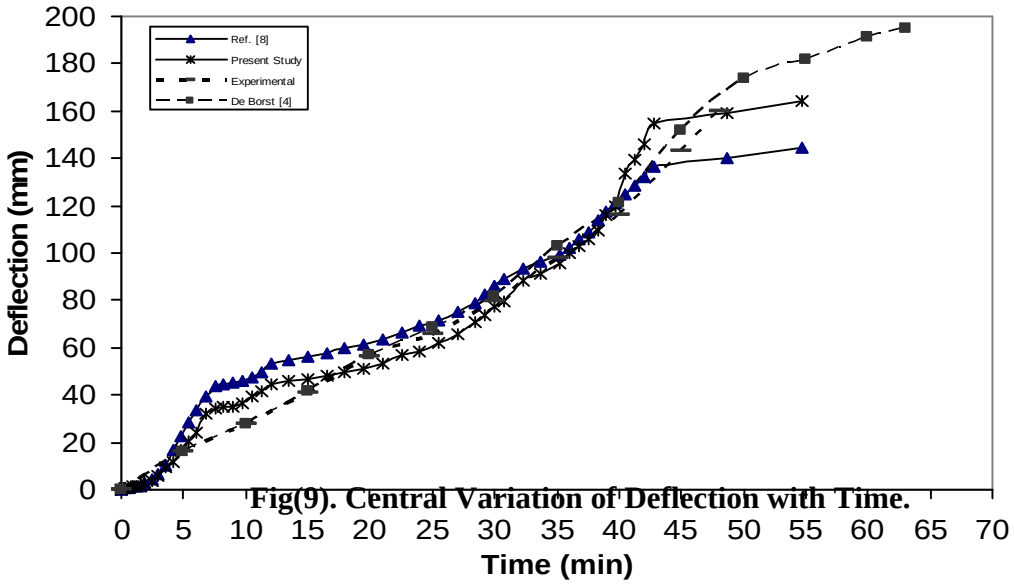

Fig(9). Central Variation of Deflection with Time.

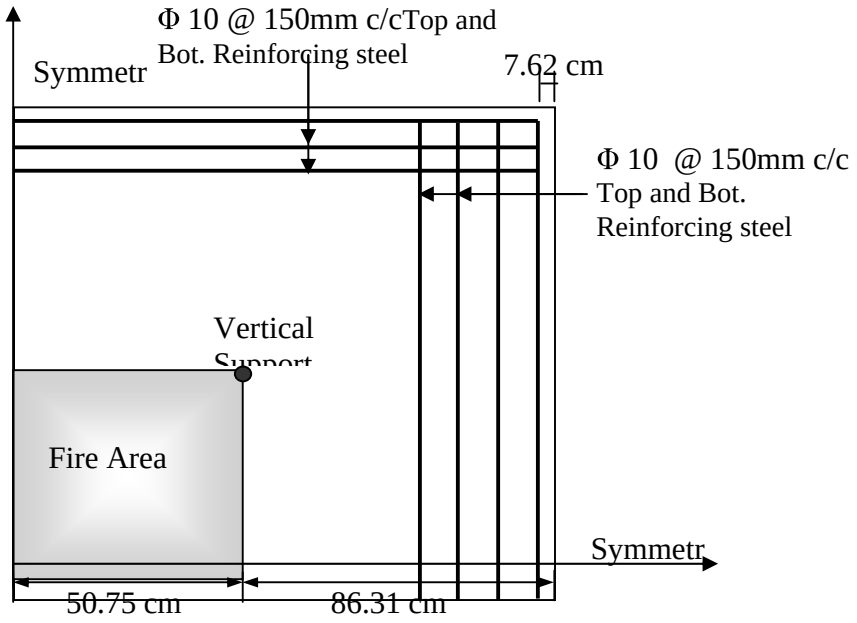

Plan View of PCA Slab

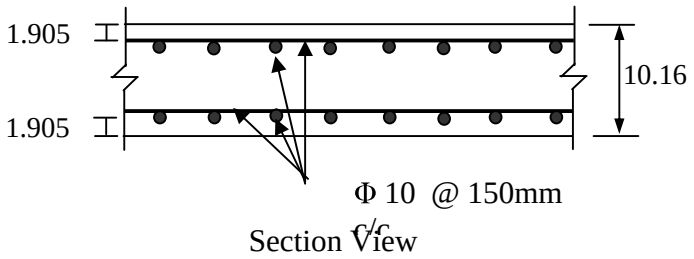

Section View

Fig.(10) Plan and Section View of PCA Slab

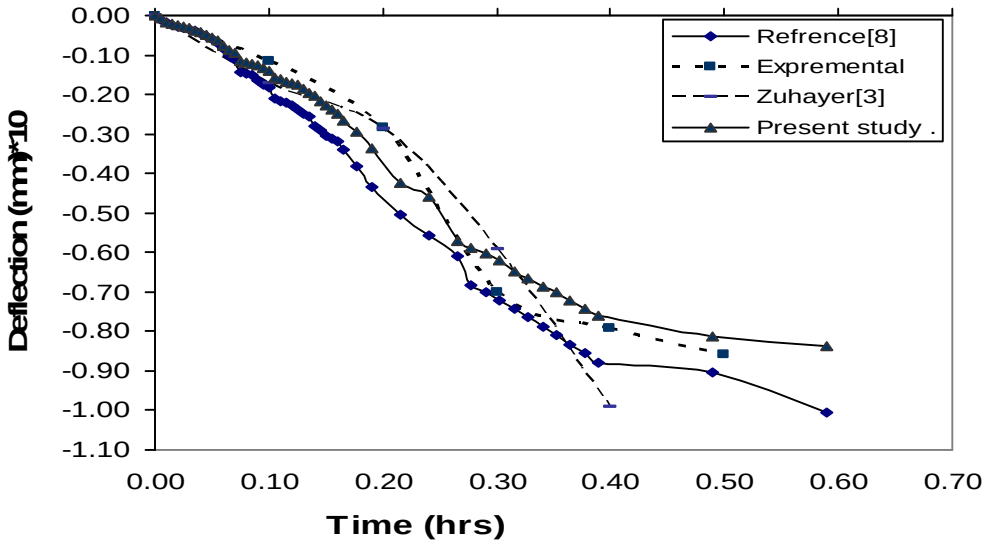

Fig(11). Variation of Deflection with Time

التحليل اللاخطي المادي والهندسي للبلاطات الخرسانية المسلحة تحت تأثير الحريق

د.أياد امجد عبد الرزاق
أستاذ مساعد
قسم الهندسة المدنية -جامعة الموصل

الخلاصة

استخدم التحليل اللاخطي بطريقة العناصر المحددة لدراسة مقاومة البلاطات الخرسانية المسلحة المتعرضة لدرجات حرارة عالية (الحرائق) ، استخدم العنصر ألصفائحي ذو العقد الثمانية للاستفادة من نظرية مندلن/ ريزنر للصفائح السميكة .

تضمن النموذج المقترح في الدراسة حالة التشقق والسحق للخرسانة وكذلك حالة الخضوع لحديد التسليح استخدم أسلوب الطبقات لتمثيل حديد التسليح كطبقة ضمن طبقات الخرسانة. استعمل أسلوب تقسيم السمك إلى طبقات لتمثيل سلوك الخرسانة خلال السمك، ان التحليل اللاخطي الهندسي يلعب دورا مهما في تحديد سلوك البلاطات الخرسانية المسلحة المتعرضة لدرجات حرارة عالية ،حيث تم صياغة السلوك اللاخطي الهندسي بنموذج رياضي استنادا الى أسلوب لاكرانج آخذا بنظر الاعتبار فرضيات فون كارمن .

تم مقارنة نتائج النموذج المقترح مع العديد من الدراسات السابقة واظهر النموذج توافقا جيدا مع النتائج العملية للدراسات السابقة.